Input Impedance of the Arterial System Using Parametric Models

Taous-Meriem Laleg, Michel Sorine, Qinghua Zhang

Input Impedance of the Arterial System Using Parametric Models

Taous-Meriem Laleg, Michel Sorine and Qinghua Zhang

Abstract— **In this work, we propose to use parametric models for the estimation of arterial tree input impedance. The results of this new method are compared with those of the standard method based on the Fast Fourier Transform (FFT). The comparison is first made with pressure and flow measurements on a calf, then with human blood pressure measurements completed by blood flow data simulated from a soliton+windkessel model. The input impedance is calculated both at aorta and finger. As illustrated by the numerical results, the advantage of the proposed parametric method is its smooth impedance estimations, whereas the standard FFT method yields more disturbed results.**

I. INTRODUCTION

Nowadays, the cardiovascular diseases constitute one of the most important causes of mortality in the world. Therefore, many studies have been devoted for modeling the cardiovascular system in order to understand and assess the behavior of this complex system both in normal and pathological cases and to develop efficiency diagnosis methods.

Like the electrical impedance defined for electrical circuits, the vascular impedance describes the relation between the arterial pressure and flow in a vessel. There are three kinds of vascular impedances [3], [9], [22] : (a) longitudinal impedance which describes the relation between the pressure drop in a vessel and the flow ; (b) the input impedance which is obtained by the blood pressure and flow measurements at the same point of the vessel ; (c) the impedance of the aorta called the characteristic impedance.

Impedance is a convenient concept for the description of linear dynamic systems through the input-output relationship. By studying the input impedance of the systemic circulation, it is implicitly assumed that the linear relationship is an sufficient approximation for the purpose of the study [13], [24]. Indeed this method has led to fruitful results for studying the characteristics of systemic arteries and the effect of physiological and pathological conditions of the arteries on the left ventricle. It can also provide information about the physical state of the arteries, an assessment of the external "after load" faced by the left ventricle and complete data for calculating the external work of the ventricle [13]. Changes in the systemic input impedance and the characteristic impedance were related to many factors such as pathological conditions and age [13].

T.M. Laleg and M. Sorine are with INRIA-Rocquencourt, B.P. 105, 78153 Le Chesnay Cedex, France. Taous-Meriem.Laleg@inria.fr, Michel.Sorine@inria.fr.

Q. Zhang is with IRISA, Campus de Beaulieu, 35042 Rennes Cedex, France zhang@irisa.fr.

Both frequency techniques and time domain methods have been proposed for input impedance estimation [6], [7], [9], [21], [22]. The standard approach is based on the Fourier analysis [9], [13], [15], [19], [24]. Blood pressure and flow are expressed as a linear superposition of sinusoidal waveforms using Fourier Transform. Only few harmonics are necessary for a good description of these waveforms.

In this article, we propose to calculate the vascular input impedance by using parametric models. In particular the ARMAX (Auto-Regressive Moving Average eXogenous input) and OE (Output Equation) models will be used. The main advantage of the model-based approach is the estimated smooth impedance. It also offers the possibility to choose noise models. In section II, we will briefly recall the basic principles of the Fourier analysis, and then in section III we will present the model-based method. Section IV contains the numerical results established from measured data. Finally, a discussion comparing the two approaches is presented in section V.

II. INPUT IMPEDANCE COMPUTED BY FFT

The relation between the arterial pressure and flow can be illustrated by Fig.1 where the arterial flow $Q(t)$ and pressure $P(t)$ are respectively considered as the input and output, $Z_{in}(t)$ denotes the impulse response of the system.

Assume that this system is linear and time invariant, then

$$P(t) = Z_{in}(t) * Q(t), \tag{1}$$

where "*" denotes the convolution. Let $\hat{Q}(\omega), \hat{P}(\omega)$ and $\hat{Z}_{in}(\omega)$ be respectively the Fourier transforms of $Q(t), P(t)$ and $Z_{in}(t)$, then equation (1) is simply written in the frequency domain as

$$\hat{P}(\omega) = \hat{Z}_{in}(\omega)\hat{Q}(\omega), \tag{2}$$

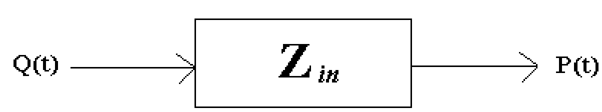

Fig. 1. Vascular input impedance.

The frequency domain notation $\hat{Z}_{in}(\omega)$ is also known as the *impedance* of the system. $\hat{Q}(\omega), \hat{P}(\omega)$ and $\hat{Z}_{in}(\omega)$ are all complex functions of the frequency ω. Usually $\hat{Z}_{in}(\omega)$ is represented by its modulus $|\hat{Z}_{in}(\omega)|$ and its phase $\phi(\omega)$:

$$\hat{Z}_{in}(\omega) = |\hat{Z}_{in}(\omega)| \exp(i\phi(\omega)). \quad (3)$$

For each harmonic, the impedance modulus is given by the ratio of the amplitudes of the pressure and flow harmonics and the phase angle by the difference between their phases :

$$|\hat{Z}_{in}(\omega)| = \frac{|\hat{P}(\omega)|}{|\hat{Q}(\omega)|}, \quad (4)$$

$$\phi(\omega) = \phi_P(\omega) - \phi_Q(\omega). \quad (5)$$

We notice that the phase is negative when the flow leads the pressure.

To calculate the pressure and flow harmonics $\hat{Q}(\omega)$ and $\hat{P}(\omega)$, typically the Fast Fourier Transform (FFT) is used. About 20 harmonics are usually sufficient for a good reconstruction of the pressure and flow signals.

Many studies have estimated the input impedance of the systemic circulation, the femoral artery and the pulmonary artery for dogs [2], [14], [15] and for men [10], [11], [13]. The forcing impedance which relates the ventricular pressure to the aortic flow was also estimated for dogs in [1] and the results were compared to the input impedance of the systemic tree. In [12], [16], [23], it has been studied the input impedance in different physiological and physiopathological conditions.

From the systemic input impedance, it is possible to find the peripheral resistance which is the value of the modulus at frequency zero and the characteristic impedance which is, in general, estimated by averaging the impedance modulus at high frequencies. Mean aortic pressure divided by mean aortic flow only gives information on peripheral resistance if, over the period of determination, the peripheral resistance does not vary.

After having calculated $\hat{P}(\omega)$ and $\hat{Q}(\omega)$ by using the FFT, the modulus and phase of the impedance can be computed, at each frequency, following equations (4) and (5). In section IV, we will present results for the input impedances at aorta level for a calf and at aorta and finger levels for a human.

Remark that the model (1) (or (2)) has been formulated under the assumption of a perfect linear relationship. In reality this model is only approximatively true, because of measurement errors and the nonlinear behavior of the system. When the computed impedance $\hat{Z}_{in}(\omega)$ is truncated to keep the lowest frequencies only, the result is equivalent to the application of a low-pass filter. In other words, such an approach assumes that modeling and measurement uncertainties are located at high frequencies only. In practice, uncertainties appear also in lower frequencies, therefore the truncated impedance often exhibits irregularities.

III. PARAMETRIC MODELS FOR IMPEDANCE ESTIMATION

In order to improve the irregular aspect of impedance estimation, in this section we propose a model-based estimation method. Inspired by the theory of linear system identification [8], ARMAX (Auto-Regressive Moving Average eXogenous input) and OE (Output Error) models will be considered. The use of such models implies two choices : rational approximation of the impulse response (or transfer function) and rational approximation of modeling and measured uncertainties (generally called *noises* as in the system identification literature). System identification generally consists of the following steps :

- Collecting input/output data.
- Choosing model structure.
- Adjusting the model parameters with a chosen cost function.

For a brief recall of linear system identification with parametric models, let us follow the typical notation of the literature : $u(t)$, $y(t)$ and $e(t)$ are respectively the input, the output and a white noise *in discrete time*. Though usually the input and output signals are continuous functions of time (like $Q(t)$ and $P(t)$). With digital signal processing techniques, continuous time signals are typically sampled at discrete time instants. For presentation simplicity, let us assume the sampling instants $t = 1, 2, 3, \ldots$. Let q be the shift operator, i.e $qu(t) = u(t+1)$ and $q^{-1}u(t) = u(t-1)$. Define the polynomial operators :

$$A(q) = 1 + a_1 q^{(-1)} + \cdots + a_{na} q^{(-na)},$$
$$B(q) = b_1 q^{(-1)} + \cdots + b_{nb} q^{(-nb)},$$
$$C(q) = 1 + c_1 q^{(-1)} + \cdots + c_{nc} q^{(-nc)},$$
$$F(q) = 1 + f_1 q^{(-1)} + \cdots + f_{nf} q^{(-nf)},$$
$$D(q) = 1 + d_1 q^{(-1)} + \cdots + d_{nd} q^{(-nd)},$$

where a_i, b_i, c_i, f_i and d_i are constant coefficients and n_a, n_b, n_c, n_f and n_d are the degrees of the polynomials. With these notations, the most commonly used parametric models are :

1) ARX (Auto-Regressive eXogenous input) : it is used when the structure has an input excitation, which is the blood flow in our case. The basic equation for the ARX model is given by :

$$y(t) = \frac{B(q)}{A(q)} u(t) + \frac{1}{A(q)} e(t). \quad (6)$$

The first term at the right hand side of this equation involves the transfer function from the input $u(t)$ to the output $y(t)$ and the second term corresponds to the noise model. The input/output and noise/output transfer functions have the same dynamic. Therefore, in this model there is no flexibility for the choice of the noise transfer function. Nevertheless, this model is frequently used for its simple estimation algorithm.

2) ARMAX (Auto-Regressive Moving Average eXogenous input) : this model is often the preferred model since it gives extra flexibility to handle disturbance with its C polynomial. The basic equation for the ARMAX model is given by :

$$y(t) = \frac{B(q)}{A(q)}u(t) + \frac{C(q)}{A(q)}e(t). \qquad (7)$$

This model has a more flexible noise transfer function with the free $C(q)$ polynomial, compared to the ARX model.

3) OE (Output Error) described by the following equation :

$$y(t) = \frac{B(q)}{F(q)}u(t) + e(t). \qquad (8)$$

This model assumes that the only uncertainty is an additive white noise, typically measurement noise.

4) BJ (Box & Jenkins) which is given by :

$$y(t) = \frac{B(q)}{F(q)}u(t) + \frac{C(q)}{D(q)}e(t). \qquad (9)$$

This model offers a better flexibility for noise transfer function, with free denominator and numerator polynomials.

The use of a rational transfer function (of moderate order) implies a regularity assumption. Consequently, the resulting impedance estimation has a smooth aspect, which will be illustrated in the following section.

In our study, we will focus on the use of ARMAX and OE models. So we propose to derive the transfer function $\hat{Z}_{in}(\omega)$ of the system described in Fig.1 using ARMAX and OE models and to compare the results to those obtained using the FFT approach.

Assume that $P(t)$ and $Q(t)$ are respectively the pressure and flow data. We suppose that the relation between $P(t)$ and $Q(t)$ can be described first by an ARMAX model then by an OE model. Therefore, we must identify the polynomials defining these structures. One of the most important aspects of the use of these models is the selection of the model order. Much work has been done by various investigators on this problem and many experimental results have been given in the literature. The purpose is to get a simple model that depends on small number of parameters and which describes the input/output behavior of the system well. The ARMAX's and OE's equations in this study are given respectively by :

$$P(t) = \frac{B(q)}{A(q)}Q(t) + \frac{C(q)}{A(q)}e(t), \qquad (10)$$

$$P(t) = \frac{B(q)}{F(q)}Q(t) + e(t), \qquad (11)$$

$A(q)$, $B(q)$, $C(q)$ and $F(q)$ are polynomials which must be identified.

After the determination of the different degrees and coefficients, we calculate the frequency response of the transfer function which is the corresponding impedance. The results are illustrated in the next section.

IV. NUMERICAL RESULTS

Calf pressure and flow measurements in the descending aorta where used. We also used blood pressure measurements for human at aortic and finger levels. The pressure at the finger has been measured using the FINAPRES device [20] and the aortic pressure has been measured using a catheter (invasive method). The human flow has been simulated with a soliton+windkessel model [4], [5].

The parameters of the predictive models were estimated using the MATLAB toolbox for identification. The identification may be done either by writing commands or by using the graphical user interface of the System Identification Toolbox. The graphical user interface is started by writing at the command prompt *ident*. To get more reliable results, it is useful to split the data into two sequences ; one for identification and one for verification. The commands *ARMAX* and *OE* can be used to estimate respectively the ARMAX and OE models. Matlab uses the least squares algorithm update the model parameters. The least square algorithm takes the model structure and input/output data from the process and estimates the model parameters. The degrees of the different polynomials of the ARMAX and OE models are presented respectively in the tables (I) and (II).

TABLE I
ARMAX MODEL

ARMAX	n_a	n_b	n_c	result (%)
Human aorta	2	2	1	85.47%
Human finger	2	2	2	90.87%
Calf aorta	4	4	3	90.26%

TABLE II
OE MODEL

OE	n_b	n_f	result (%)
Human aorta	2	2	86.29%
Human finger	2	2	91.91%
Calf aorta	4	5	94.37%

We notice that a two degree model is sufficient for a good reconstruction of the human pressure. This result is in agreement with the 4-element windkessel model [18]. For the Calf data, we obtain a fourth order model.

The figures (2)-(16) illustrate the reconstructed pressure and the input impedance using the FFT approach, the ARMAX and OE models at calf aorta, human aorta and at human finger respectively.

We notice that the shape of the input impedance obtained are similar to the examples published previously [9], [13], [15]. The modulus is high at low frequencies then decreases rapidly to be constant at higher frequencies. On the other hand, the phase is negative at low frequencies (denoting that flow leads pressure) and increases at higher frequencies [9], [13].

The shape of the input impedance can be explained by the windkessel theory [17], [22]. For a resistant flow, the phase angle is zero and the amplitude constant. For a compliant artery, the flow is advanced with respect to pressure, it behaves like an integrator with a decrease in the amplitude and a phase equals to -90°. For an inertance, the flow is delayed, the amplitude increases and the phase is equal to +90°. In the case of large arteries like aorta where we define the characteristic impedance, the mass effects and compliance interact in such a way that the pressure and flow waves are in phase and their ratio is constant. This means that large vessels behave like a resistance.

The estimated input impedances by the two approaches look very similar at the finger level but some differences are noticed at aorta particularly in high frequencies. This can be due to the errors of measurements. It is noticed also that the parametric models give smooth estimation comparing to the FFT-based approach.

V. CONCLUSION

Because the concept of impedance has been originally defined in the frequency domain, it is natural to use FFT for

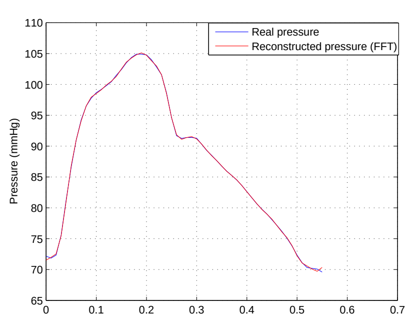

Fig. 2. Reconstructed calf pressure at the aorta level using the FFT approach.

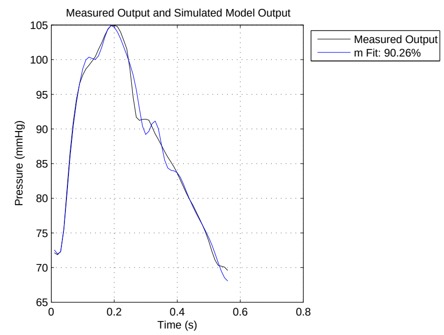

Fig. 3. Reconstructed calf pressure at the aorta level using an ARMAX model.

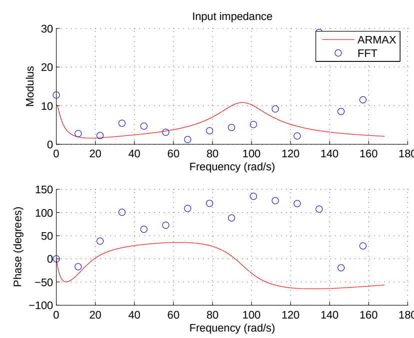

Fig. 4. Input impedance at the calf aorta : ARMAX and FFT approaches.

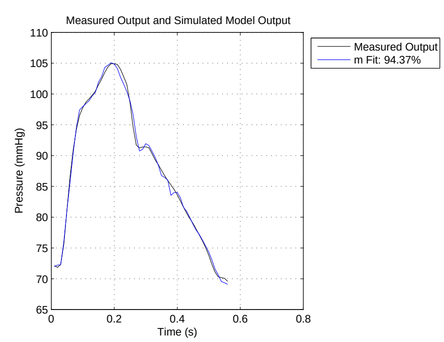

Fig. 5. Reconstructed calf pressure at aorta level using an OE model.

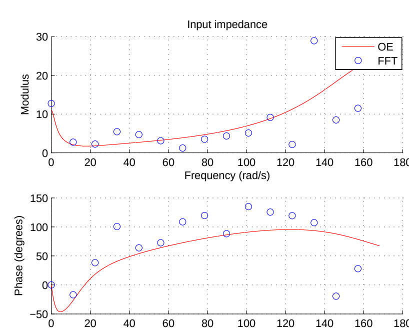

Fig. 6. Input impedance at calf aorta : OE and FFT approaches.

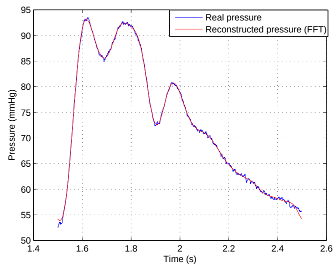

Fig. 7. Reconstructed human pressure at the aorta level using the FFT approach.

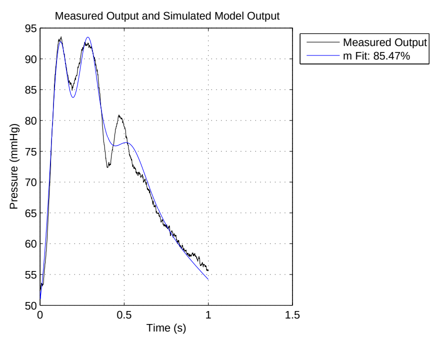

Fig. 8. Reconstructed human pressure at the aorta level using an ARMAX model.

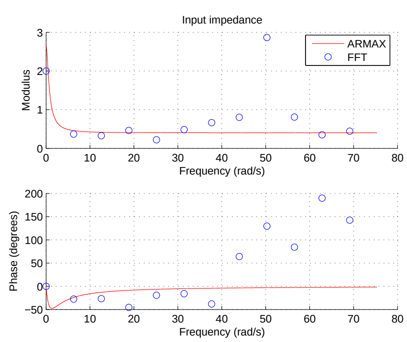

Fig. 9. Input impedance at human aorta : ARMAX and FFT approaches.

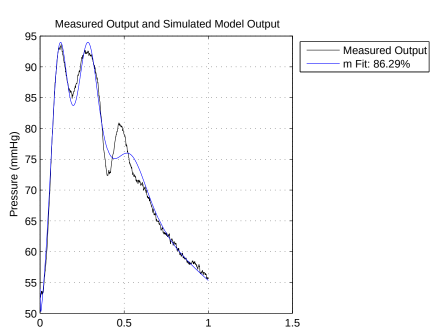

Fig. 10. Reconstructed human pressure at the aorta level using an OE model.

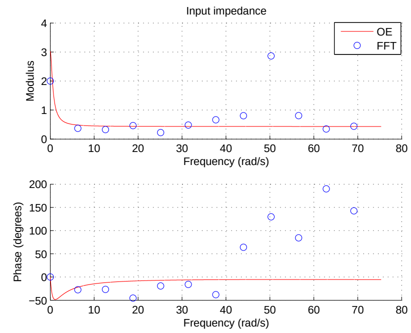

Fig. 11. Input impedance at human aorta : OE and FFT approaches.

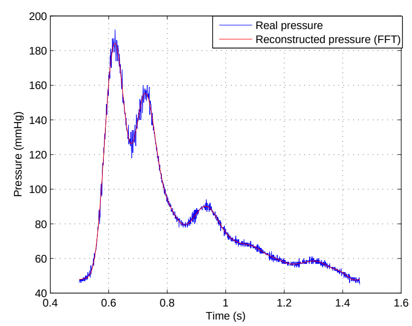

Fig. 12. Reconstructed human pressure at the finger level using the FFT approach.

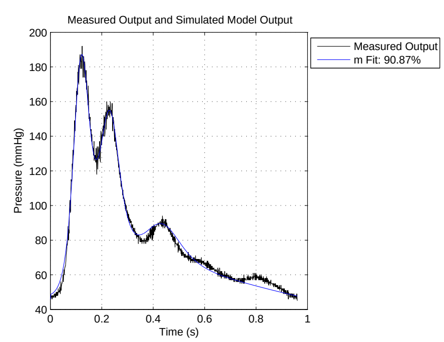

Fig. 13. Reconstructed human pressure at the finger level using an ARMAX model.

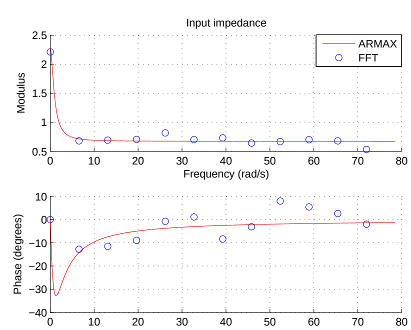

Fig. 14. Input impedance at human finger : ARMAX and FFT approaches.

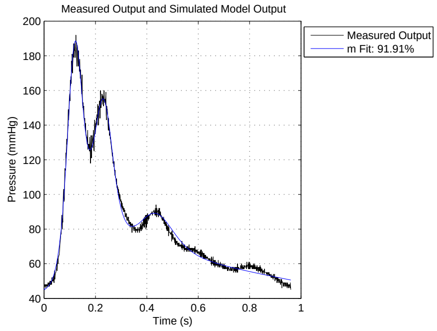

Fig. 15. Reconstructed human pressure at the finger level using an OE model.

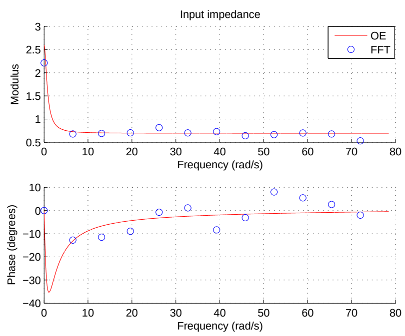

Fig. 16. Input impedance at human finger : OE and FFT approaches.

its estimation. However, due to modeling and measurement uncertainties, the impedance estimated by FFT has an irregular aspect. The application of frequency domain filtering (with low-pass or band-pass filters) corresponds to the truncation of certain frequency components, thus not efficient in presence of large band disturbances. On the other hand, the model-based methods produce more smooth impedance estimation and provides a simple interpolation for continuous spectral estimation. However, this method is more time consuming than the FFT based method.

References

[1] F.L. Abel. Fourier analysis of left ventricular performance evaluation of impedance matching. *Circulation Research*, (28) :119–135, 1971.

[2] DH. Bergel and WR. Milnor. Pulmonary vascular impedance in the dog. *Circulation Research*, 16 :401–415, 1965.

[3] E.P. D'Alché. *Comprendre la Physiologie Cardiovasculaire*. Médecine-Sciences Flammarion, 2^{nd} edition, 2003.

[4] T.M. Laleg, E. Crépeau, and M. Sorine. Arterial pressure modelling by an integrable approximation of navier-stokes equations. In *5th Mathmod Vienna Proceedings*, volume 1, page 337. ARGESIM Report, February 2006.

[5] T.M. Laleg, E. Crépeau, and M. Sorine. Separation of arterial pressure into solitary waves and windkessel flow. *submitted to MCBMS'06, 6th IFAC Symposium on Modelling and Control in Biomedical Systems, Reims (France)*, September 2006.

[6] J.K.J. Li. Cardiovascular diagnostic parameters derived from pressure and flow pulses. *IEEE Frontiers of Engineering in Health Care*, pages 531–534, 1982.

[7] J.K.J. Li. Time domain resolution of forward and reflected waves in the aorta. *IEEE Transactions on Biomedical Engineering*, 33(8) :783–785, 1986.

[8] L. Ljung. *System Identification : Theory for the User*. Prentice Hall, 2^{nd} edition, 1999.

[9] D.A. McDonald. *Blood flow in arteries*. Edward Arnold, 2^{nd} edition, 1974.

[10] W.R. Milnor and M.F. O'Rourke C.R. Conti, K.B. Lewis. Pulmonary arterial pulse wave velocity and impedance in man. *Circulation Research*, 25 :637–649, 69.

[11] JP. Murgo and N. Westerhof. Input impedance of the pulmonary arterial system in normal man. effects of respiration to systemic impedance. *Circulation Research*, 54 :666–673, 1984.

[12] JP. Murgo, N. Westerhof, JP. Giolma, and SA. Altobelli. Effects of exercise on aortic input impedance and pressure wave forms in normal humans. *Circulation Research*, 48 :334–343, 1981.

[13] WW. Nichols, CR. Conti, WE. Walker, and WR. Milnor. Input impedance of the systemic circulation in man. *Circulation Research*, 40 :451–458, 1977.

[14] M.F. O'Rourke and M.G. Taylor. Vascular impedance of the femoral bed. *Circulation Research*, (18) :126–139, 1966.

[15] M.F. O'Rourke and M.G. Taylor. Input impedance of the systemic circulation. *Circulation Research*, (4) :365–380, 1967.

[16] CJ. Pepine, WW. Nichols, and Conti CR. Aortic input impedance in heart failure. *Circulation Research*, 58(3) :460–465, 1978.

[17] N. Stergiopulos, P. Segers, and N. Westerhof. Use of pulse pressure method for estimating total arterial compliance in vivo. *The American Physiological Society*, (276) :424–428, 1999.

[18] N. Stergiopulos, B.E. Westerhof, and N. Westerhof. Total arterial inertance as the fourth element of the windkessel model. *The American Physiological Society*, pages 81–88, 1999.

[19] M.G Taylor. Use of random excitation and spectral analysis in the study of frequency-dependent parameters of the cardiovascular system. *Circulation Research*, 18 :585–595, 1966.

[20] K.H. Wesseling. Method and device for controlling the cuff pressure in measuring the blood pressure in a finger by means of photo-electric plethysmograph. *United State Patent*, September 1985.

[21] N. Westerhof, P. Sipkema, G.C. Van Den Bos, and G. Elzinga. Forward and backward waves in the arterial system. *Cardiovascular Research*, 6 :648–656, 1972.

[22] N. Westerhof, N. Stergiopulos, and M.I.M. Noble. *Snapshots of Hemodynamics, An Aid for Clinical Research and Graduate Education*. Springer Science, 2005.

[23] F.C.P. Yin and W.R. Milnor M.L. Weisfeldt. Role of aortic input impedance in the decreased cardiovascular response to exercise with aging in dogs. *The American Society for Clinical Investigation*, 68 :28–38, July 1981.

[24] M. Yoshigi and BB. Keller. Linearity of pulsatile pressure-flow relations in the embryonic chick vascular system. *Circulation Research*, 79 :864–870, 1996.